Measurement of the form factors in the decay $K^+ \to \pi\mu\nu$ †

C. L. Arnold, B. P. Roe, and D. Sinclair
Physics Department, University of Michigan, Ann Arbor, Michigan 48104
(Received 14 September 1973)

By studying K^+ stopping in a Freon bubble chamber, we have measured the slopes of the vector and scalar form factors in the decay $K^+ \to \pi\mu\nu$, and find them to be $\lambda_+ = 0.025 \pm 0.03$, $\lambda_0 = -0.04 \pm 0.04$. This result is in good agreement with other experiments on $K^+_{\mu 3}$ decays, but not in agreement with the predictions of current algebra. It disagrees with the result of a recent high-statistics experiment on $K^0_{\mu 3}$ decays.

I. INTRODUCTION

We have studied the $K^+_{\mu 3}$ decay of the K^+ meson, $K^+ \to \mu^+ + \pi^0 + \nu$, by observing K^+ mesons come to rest in a 40-in. bubble chamber filled with Freon (C_2F_5Cl). The purpose of our study was a measurement of the $K^+_{\mu 3}$ form factors and our answer is based on a final sample of 490 events.

Under certain assumptions, the distribution of events on the $K_{\mu 3}$ Dalitz plot can be calculated in terms of two form factors which are functions of t, the square of the four-momentum transferred to the leptons.[1] The distribution is of the form

$$\rho(E_\pi, E_\mu) = f_+^2 A + f_+ f_- B + f_-^2 C, \tag{1.1}$$

where f_+ and f_- are the form factors, and A, B, and C are functions of the kinematic quantities and are derived from the theory. It is usual to expand f_+ and f_- as polynomials in t and to retain only the first-order term. Thus

$$f_\pm(t) = f_\pm(0)\left(1 + \lambda_\pm \frac{t}{m_\pi^2}\right), \tag{1.2}$$

where m_π is the mass of the pion.

In principle, a measurement of the distribution $\rho(E_\pi, E_\mu)$ would enable one to determine λ_+, λ_-, and the ratio $f_-(0)/f_+(0)$, usually denoted by $\xi(0)$. In fact, however, the factors B and C are considerably smaller than A except in the region of low pion energy (i.e., high t). Thus unless one does a very high-statistics experiment, which this is not, one gets virtually no information on the t dependence of ξ but only a measure of its value averaged over the high-t region of the Dalitz plot. The usual procedure is to remove the parameter λ_- by setting it equal to zero.

Theoretical predictions of the form factors are concerned with the two amplitudes corresponding to spin-parity exchanges of 1^- and 0^+ between the K and the π. The 1^- amplitude is simply equal to f_+. The 0^+ amplitude, $f_0(t)$, is related to f_+ and f_- as follows:

$$f_0(t) = f_+(t) + \frac{t}{m_K^2 - m_\pi^2} f_-(t). \tag{1.3}$$

Keeping only terms linear in t, f_0 may be developed as

$$f_0(t) = f_0(0)\left(1 + \lambda_0 \frac{t}{m_\pi^2}\right). \tag{1.4}$$

If $f_-(0)$ is finite then $f_0(0) = f_+(0)$. By dividing Eq. (1.3) by f_+ and then making the substitutions given in Eqs. (1.2) and (1.4) and setting $\lambda_- = 0$, one obtains the relation

$$\lambda_0 = \lambda_+ + \frac{m_\pi^2}{m_K^2 - m_\pi^2}\xi(0). \tag{1.5}$$

Theoretical predictions,[2] based on the soft-pion formalism,[3] and assuming $f_0(t)$ to be a reasonably smooth and monotonic function in the physical region, indicate that λ_0 should be positive with a value ~0.02. Though there are some experimental results[4,5] in agreement with this prediction, there are many experimental data[2,6,7] which indicate a negative value for λ_0, and this experiment adds additional weight to that result.

II. EXPERIMENTAL PROCEDURES

K^+ mesons, produced on an internal target of the Argonne ZGS, were stopped in the Michigan-Argonne 40-in. bubble chamber[8] filled with Freon (C_2F_5Cl). The chamber was inside a magnet which provided a field of 45 kG normal to the viewing window. Approximately 250 000 pictures were taken, with an average of ~3 K^+ stopping in each picture.

A. Scanning and event selection

The pictures were scanned using projectors fitted with digitized measuring stages, which were on-line to a small computer. This allowed the scanners to make simple tests, such as measuring the length of a secondary track, and get an immediate answer from the computer.

The scanners were instructed to area-scan the film for positron-electron pairs or Compton electrons pointing to a discontinuity, either of direction or bubble density, in an incoming track. In the following description we refer to this discontinuity as the *stopping point* even though no attempt was made at the scanning stage to exclude decays in flight. Furthermore, we use the term *electron pairs* to include both Compton electrons and positron-electron pairs.

Events were selected for rough measurement if there were at least two electron pairs pointing to the stopping point and the stopping point was within a fiducial volume corresponding to a central region of the chamber. The rough measurement consisted of measuring the stopping point, the apex of each electron pair, and four points along the secondary track, including the end point. These measurements were made on each of two stereo views. Events were subjected to fine measurement only if they passed the following tests:

(a) At least two of the electron pairs had dip angles less than 55°, directions differing by more than 56°, and conversion distances greater than 1.3 cm.

(b) The dip angle of the secondary track was less than 55°.

(c) The range of the secondary track was between 10.7 cm and 31.0 cm, or greater than 35.0 cm.

The main purpose of these cuts was to eliminate most of the $K_{\pi 2}$ and $K_{\pi 3}$ decays before investing the effort necessary for a finer measurement. They also eliminated steeply dipping tracks.

Events passing the tests described above were measured on three stereo views to determine the direction of the primary track, the direction and range of the secondary track, and the direction and curvature of each of the tracks in the electron pairs. The geometry reconstruction program SHAPE was used to compute these quantities and their errors.

The events which were processed through SHAPE were now subjected to range and dip cuts similar to, but slightly tighter than, those used after the rough measurement. The range of the secondary was required to be either in the interval 11.3 cm to 28.0 cm or in the interval 35 cm to 52 cm. The dip of the secondary was required to be less than 47.5° and the dip of each electron pair to be less than 50°. The angle between the directions of the two electron pairs was required to be greater than 63°. As a result of these cuts the sample was reduced to 2276 events.

TABLE I. Effects of various tests on the sample size.

Number passing range, dip, and opening-angle cuts	2276
Number passing physicists' edit scan	956
Number passing test for large measurement errors	842
Number passing test for stray electron pairs	801
Number passing test for $K_{\pi 2}$ decays at rest	595
Number which reconstruct as $K_{\mu 3}$ decay at rest	490

These events were then examined by physicists to check on the following points:

(1) that the point measured as the stopping point was indeed the end of a track whose bubble density was consistent with that of K^+ coming to rest;

(2) that the secondary track had no sharp discontinuities in either bubble density or direction indicative of a nuclear interaction; and

(3) that the electron pairs did indeed point to the stopping point and did not have some other suitable origin in the picture.

As a result of these checks, the sample size was reduced to 956. These events were now subjected to several tests using the output data from the geometry measurements. The tests are described below and their effects on the sample size are shown in Table I. Their purpose was to remove from the sample events with abnormally large measuring errors and also to remove as much as possible two of the contaminants remaining in the sample, namely

(1) $K_{\pi 2}$ decays at rest in which the pion underwent a nuclear interaction that was not detected by the physicists' scan and

(2) events in which one (or both) electron pair was not associated with the event but was from another source, though it pointed to the stopping point well enough to pass visual inspection.

The tests applied were as follows.

1. Test for large measurement errors. We placed the following requirements on the errors calculated by the SHAPE geometry program:

$$|\Delta E_\gamma| \leq 0.25 E_\gamma \text{ for } E_\gamma \leq 60 \text{ MeV},$$

$$|\Delta E_\gamma| \leq 0.18 E_\gamma \text{ for } E_\gamma > 60 \text{ MeV},$$

$$|\Delta\Phi| \leq 1.34 |\Delta\Phi|_{\text{av}},$$

$$|\Delta p_\mu| \leq 1.2 |\Delta p_\mu|_{\text{av}}.$$

E_γ is the energy of the electron pair, p_μ is the momentum of the secondary track, and Φ is the azimuthal angle of the secondary track. $|\Delta\Phi|_{\text{av}}$ and $|\Delta p_\mu|_{\text{av}}$ are average errors and are empirical functions of each track's momentum and dip.

2. Test for stray electron pairs. We required that each electron pair point to the stopping point and we used the following criterion:

$$\frac{(\varphi_\gamma - \varphi_L)^2}{\Delta\varphi_\gamma{}^2} + \frac{(\lambda_\gamma - \lambda_L)^2}{\Delta\lambda_\gamma{}^2} \leq 25. \qquad (2.1)$$

φ and λ are, respectively, the azimuthal and dip angles, and the subscripts γ and L, respectively, refer to the electron pair and to the line joining the apex of the electron pair to the stopping point. We also required that the invariant mass of the two electron pairs be consistent with that of a pion, by using the following criterion:

$$\left(\frac{M_{\gamma\gamma} - M_\pi}{\Delta M_{\gamma\gamma}}\right)^2 \leq 2.25 . \tag{2.2}$$

3. Test for $K_{\pi 2}$ decays at rest. $K_{\pi 2}$ decays at rest have the property that the directions of the two γ rays from the π^0 and the π^+ direction are coplanar. It is also required that $\cos\eta/\cos\xi = 0.835$, which is the velocity of the π^0 from a $K_{\pi 2}$ decay. ξ is the angle between the π^0 direction and the bisector of the two γ-ray directions, and η is half the angle between the γ-ray directions. These conditions can be tested without reference to the energies of the charged secondary or the γ rays. We required that

$$\left(\frac{\epsilon}{\Delta\epsilon}\right)^2 + \left(\frac{\beta - 0.835}{\Delta\beta}\right)^2 > 11 , \tag{2.3}$$

where ϵ is the coplanarity angle and $\beta = \cos\eta/\cos\xi$.

B. $K_{\mu 3}$ Reconstruction

The 595 events which survived the cuts described in Sec. II A were put into a $K_{\mu 3}$ reconstruction program. The kinematic quantities in the $K_{\mu 3}$ decay at rest may be reconstructed from measurements of the muon energy and direction, and only the directions of the γ rays. These quantities are fairly accurately known compared to the γ-ray energies, which have large errors. However, the reconstruction using only the four quantities mentioned above gives a quadratic equation with two solutions, and information about the γ-ray energies is needed to determine which solution has the higher probability of being correct.

We calculated the energies and associated errors of the two γ rays by reconstructing the $K_{\mu 3}$ decay from the four measured quantities described above. We then used the directly measured values of the γ-ray energies and their errors to calculate a χ^2 for each of the two solutions. The solution with the higher χ^2 was rejected and the other one was retained for our analysis. Figure 1(a) is a histogram of the fractional difference in γ-ray energies between the two solutions. This should be compared with Fig. 1(b), which is a histogram of the fractional difference between the γ-ray energy predicted by the best solution and the measured γ-ray energy.

For some events (149), the discriminant in the quadratic equation was negative. There are two possibilities when this occurs. One is that the event has a $K_{\mu 3}$-decay configuration in which the two solutions occur fairly close to one another (discriminant near zero) and measuring errors cause the discriminant to go negative. The other possibility is that the event is not a $K_{\mu 3}$ decay at rest.

The procedure we adopted for the events with negative discriminants was to perturb the four measured quantities, which are the input to the calculation, by plus and minus one standard error, and go through the computation for each combination of errors. Each event was thus computed 3^4 times. Of the 149 events with negative discriminants, 105 persisted with negative discriminants in all of the 81 combinations of errors tried. Monte Carlo studies showed that these events are virtually all contaminants, that is, not $K_{\mu 3}$ decays at rest.

The events which gave solutions for some of the 81 combinations tried were accepted as $K_{\mu 3}$ decays at rest. The γ-ray energies were calculated for each solution of each error combination and an average was found along with a standard deviation. This was used along with the directly measured γ-ray energies to determine a χ^2 for each solution. The solution with the lower χ^2 was accepted and the other was rejected. The 490 events for which

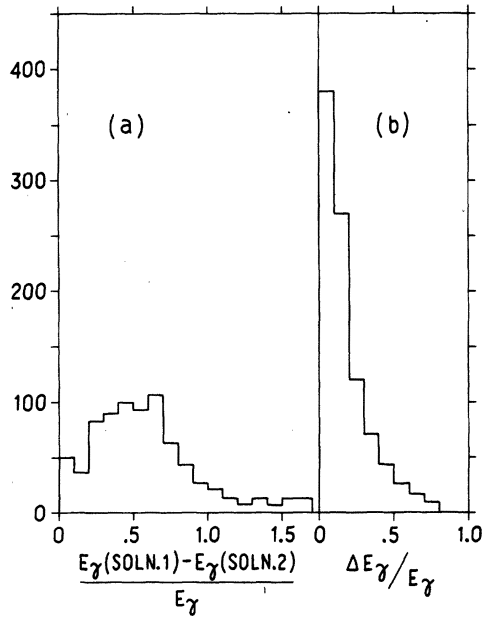

FIG. 1. (a) The difference in γ-ray energies between the two solutions as a fraction of E_γ corresponding to the best solution. There are 116 events off scale to the right. (b) The difference in γ-ray energies between the best solution and the directly measured value, as a fraction of E_γ. Each $K_{\mu 3}$ decay contributes two events to each histogram.

solutions were possible form the final sample on which our measurement of $\xi(0)$ and λ_+ is based.

The reader might ask why the procedures described above were used instead of the well-known method of χ^2 fitting. Using this method, each event would be in a constraint class greater than 0C if the γ-ray energies were included as measured parameters. All the variables could then be adjusted to minimize χ^2 while satisfying the constraint equations. The reason this approach was not used is the following: The γ-ray energies have relatively large errors, their median value being about 8%. This should be compared with errors in muon momentum of about 2% median value. Furthermore, the fraction of impurities in the sample to be fitted is large. Under these circumstances many events will not converge to a fit and there will be many more for which the fit is bad.

As a check on our procedure of rejecting all 105 events which failed to reconstruct as $K_{\mu 3}$ decays at rest, we estimated the number of impurities in our sample of 595 events (see Sec. II D). We then

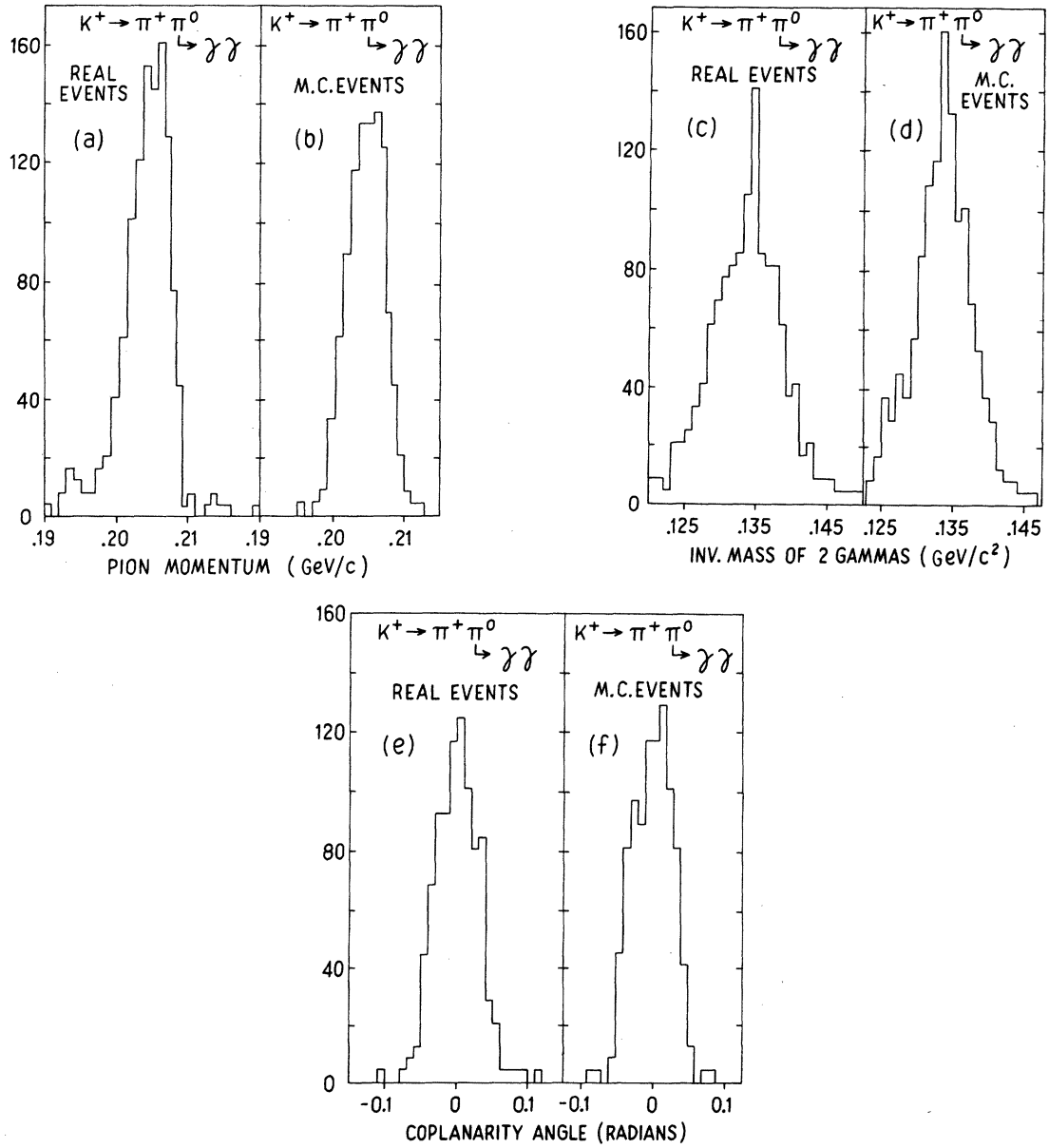

FIG. 2. Shown for comparison are histograms of pion momentum, 2γ invariant mass, and coplanarity angle. (a), (c), and (e) were drawn using data from real $K_{\pi 2}$ decays at rest. (b), (d), and (f) were drawn using data from fake $K_{\pi 2}$ decays at rest constructed by our Monte Carlo program.

computed by a Monte Carlo calculation how many of these impurities would fail to reconstruct as $K_{\mu 3}$ decays at rest. We obtained an answer of 56 events. Then we estimated by Monte Carlo calculation that 39 $K_{\mu 3}$ decays at rest would fail to reconstruct. The total estimate of failures was thus 95, which is in agreement with the actual number of 105.

C. Monte Carlo simulation of the events

The method used to determine the parameters $\xi(0)$ and λ_+, as described in Sec. II E, was to compare the experimental data, with all its cuts and biases, to a set of events produced by the computer with the same cuts and biases. To do this we constructed a Monte Carlo program which simulated our experimental sample of $K_{\mu 3}$ events with respect to measurement errors, scanning bias, effects of chamber geometry, and impurities. To this sample we applied the same cuts used on the experimental sample and described in Secs. II A and II B.

1. *Measurement errors*

The Monte Carlo events had their kinematic parameters smeared in a way which corresponded to the distribution of errors given by the geometry program SHAPE. The SHAPE errors were, in turn, adjusted and checked by measuring a sample of $K_{\pi 2}$ decays at rest. Figures 2(a)–2(f) show the results of this check. In Figs. 2(a) and 2(b), we plot a histogram of the momentum of the charged secondary from a sample of measured $K_{\pi 2}$ events and from a sample of simulated $K_{\pi 2}$ events. In Figs. 2(c) and 2(d) we do the same thing for the invariant mass of the two γ rays, while in Figs. 2(e) and 2(f) we do it for the coplanarity angle ϵ. In each case the error distribution for the simulated events corresponds closely to that for the real events except for the tails of the distributions. However, when the cuts on large errors are applied to each sample as described in Sec. II A this discrepancy disappears.

2. *Scanning bias*

The probability of finding an electron pair is correlated with its energy. This in turn distorts the pion energy spectrum. To measure this scanning bias we deliberately "turned off" the range test, applied at the scanning stage to the charged secondary, for a randomly chosen sample of events. In this way we obtained a measured sample of $K_{\pi 2}$ events selected in precisely the same manner as our $K_{\mu 3}$ events. Figure 3 shows the energy distribution of the lower-energy electron pair (a) from measured $K_{\pi 2}$ decays and (b) from $K_{\pi 2}$ decays simulated by the Monte Carlo program which included a suitably chosen efficiency function. The function used is

$$S = 25(E_\gamma - 0.011) \text{ for } E_\gamma \leq 0.051 \text{ GeV},$$
$$S = 1.0 \text{ for } E_\gamma > 0.051 \text{ GeV}. \tag{2.4}$$

3. *Impurities*

The percentages of contaminants in the final sample of 490 events are estimated in Sec. II D. These estimates are the following.

$K_{\mu 3}$ decays in flight: 0.8%,

$K_{\pi 2}$ decays in flight: 2.1%,

$K_{\mu 3}$ decays with one stray γ ray: 2.6%.

Events of these types were simulated by the Monte Carlo program and subjected to the same cuts as our experimental sample. The events passing the cuts were then added to our final sample of simulated $K_{\mu 3}$ decays at rest in the percentages prescribed above.

4. *Effects of chamber geometry*

Low-energy muons have a better chance of stopping in the chamber than high-energy muons. Because of the relatively large dimensions of the chamber (1.03 m in diameter by 0.63 m deep) and

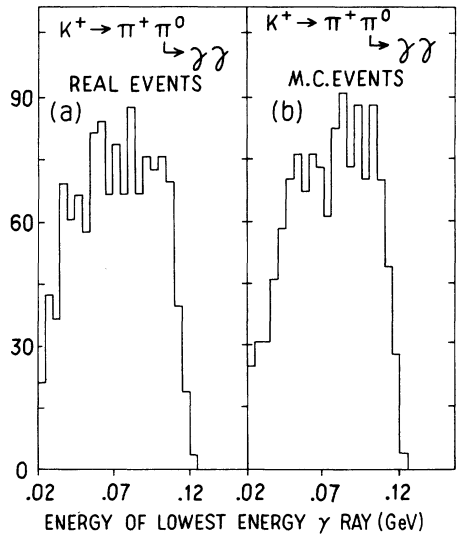

FIG. 3. Shown for comparison are histograms of the energy of the lowest-energy γ ray, (a) from real $K_{\pi 2}$ decays at rest and (b) from fake $K_{\pi 2}$ decays at rest which were generated by the Monte Carlo program. The dropoff below 0.05 GeV is the result of a scanning bias in the case of real events, and a suitably chosen efficiency function in the case of fake events.

the trapping effect of the magnetic field, the bias introduced by this effect is fairly small, being 6% for the highest-energy muons and zero for the lowest. This bias was included in our Monte Carlo simulation.

D. Estimation of the impurities in the final sample

Possible contaminants in the final sample, which we considered in detail, were the following:

(1) $K_{\mu 3}$ decays in flight,

(2) $K_{\pi 2}$ decays in flight,

(3) $K_{\mu 3}$ decays with one stray γ ray.

A fourth possibility, τ' decays in flight, was estimated to be less of a contaminant than the $K_{\mu 3}$ decays in flight and hence negligible, and the tests for $K_{\pi 2}$'s at rest are so restrictive (see Sec. II A) that they completely eliminate this mode from the final sample.

The probability of a K^+ meson which has entered the fiducial volume turning up in our final sample as a $K_{\mu 3}$ at rest is given by

$$P(K_{\mu 3} \text{ at rest}) = F_B F_R F_E F_C , \tag{2.5}$$

where F_B = the branching fraction for the $K_{\mu 3}$ mode, F_R = the fraction which come to rest, F_E = the fraction which produce two electron pairs that are found by the scanner, and F_C = the fraction which pass all cuts and reconstruct as a $K_{\mu 3}$ at rest. The probability of a K^+ meson which has entered the bubble chamber turning up in our final sample as a $K_{\mu 3}$ *in flight* is given by

$$P(K_{\mu 3} \text{ in flight}) = F_B F_F F_E F_C , \tag{2.6}$$

where F_F = the fraction which decay in flight with momentum less than 350 MeV/c. A similar expression can be written for the probability of a $K_{\pi 2}$ in flight turning up in the final sample. The stipulation that the in-flight momentum be less than 350 MeV/c is there because it was determined that kaons decaying with momenta greater than 350 MeV/c would have been recognized as in-flight decays by the physicists' scan (see Sec. II A).

The estimates of these fractions are given in Table II, except F_E, which is only crudely known to be ~0.2, but which is essentially the same for each of the three modes. The branching fractions were taken from the table of the Particle Data Group[9]; F_R and F_F are readily calculated from the K^+ lifetime and the mean stopping length in the chamber. The F_C's for each of the modes were determined from Monte Carlo simulation of the decays. From the figures in Table II the following estimates of contaminants in the final sample are readily obtained:

$$\frac{K_{\pi 2} \text{ in flight}}{K_{\mu 3} \text{ at rest}} = \frac{1.2\times10^{-4}}{56\times10^{-4}} = 0.022 ,$$
$$\frac{K_{\mu 3} \text{ in flight}}{K_{\mu 3} \text{ at rest}} = \frac{0.5\times10^{-4}}{56\times10^{-4}} = 0.009 . \tag{2.7}$$

To estimate the other major contaminant in our final sample, namely $K_{\mu 3}$ decays with one stray electron pair, we selected events which, on the basis of their secondaries' ranges, were $K_{\pi 2}$ decays at rest. The events in the sample for which the electron pairs did not pass the same criteria as were applied to the $K_{\mu 3}$ sample were eliminated. Then the test for a $K_{\pi 2}$ decay at rest (see Sec. II A) was applied to each of the 250 events in the sample. 17 events failed to pass the test, which indicated that they were probably not $K_{\pi 2}$ decays at rest. 14 of these were certainly not $K_{\pi 2}$ decays at rest. The other three came close to fitting. The probability that an event with a stray electron pair would reconstruct as a $K_{\pi 2}$ at rest is ~2%, corresponding to less than one event. Thus our estimate is that ~17 events in the sample are not $K_{\pi 2}$ decays at rest. A Monte Carlo calculation indicated that ~6 $K_{\mu 3}$ decays out of our sample of 250 events would have secondaries in the $K_{\pi 2}$ range slice. Thus it could be inferred that ~11 of the 250 events had one stray electron pair. Our $K_{\mu 3}$ sample of 595 events could be expected to contain events with stray electron pairs in the same ratio (4%), or 25 events.

$K_{\mu 3}$ events in which one electron pair is a stray will not always reconstruct as $K_{\mu 3}$ decays at rest. A Monte Carlo study showed that only 52% of these events reconstructed. Thus we expect our final sample of 490 events to contain ~13 events (2.6%) with one stray electron pair. This number has a fairly large error. Taking account of statistical errors and the possibility that 3 of the 17 events which failed the $K_{\pi 2}$ test were nonetheless $K_{\pi 2}$ decays, we place the estimate of stray γ impurities at between 1% and 3.7%.

E. Determination of $\xi(0)$, λ_+, and λ_0

We determined the parameters $\xi(0)$ and λ_+ by comparing the distribution of events in our experimental sample with distributions computed by our Monte Carlo program using different values of

TABLE II. Estimates of the fractions involved in Eqs. (2.5) and (2.6).

	F_B	F_R or F_F	F_C	Product
$K_{\mu 3}$ at rest	0.034	0.82	0.20	56×10^{-4}
$K_{\pi 2}$ in flight	0.208	0.077	0.0076	1.2×10^{-4}
$K_{\mu 3}$ in flight	0.034	0.077	0.019	0.5×10^{-4}

these parameters. The variables in which the distributions were calculated were not those of the Dalitz plot. Instead we used the variables $\cos\beta$ and V. β is the angle between the pion and the muon in the π-ν rest system. V is the invariant mass of the π-ν system, in GeV. The distribution $\rho(\cos\beta, V)$ has the nice property[10] that it is almost linear in $\cos\beta$ because λ_+ is small. The expression for ρ is as follows:

$$\rho(\cos\beta, V) = F(A + B\xi + C\xi^2), \tag{2.8}$$

where

$$F = \left(1 + \frac{\lambda_+ t}{m_\pi^2}\right)^2 (V^2 - M_K^2)\, p_\mu / V^3,$$

$$\xi = \xi(0)\left(1 + \frac{\lambda_+ t}{m_\pi^2}\right)^{-1},$$

$$A = V^2(4m_K^2 + 3m_\mu^2 - 4V^2) + m_\mu^2(M_K^2 - m_\mu^2) + 2m_K p_\mu \cos\beta(4V^2 - m_\mu^2), \tag{2.9}$$

$$B = 2m_\mu^2(3V^2 + m_K^2 - m_\mu^2) - 4m_\mu^2 m_K p_\mu \cos\beta,$$

$$C = m_\mu^2(m_K^2 - m_\mu^2 - V^2) - 2m_\mu^2 m_K p_\mu \cos\beta,$$

$$t = m_\mu^2 + (V^2 - m_\pi^2) \times (m_K^2 - m_\mu^2 - V^2 - 2m_K p_\mu \cos\beta)/2V^2,$$

$$p_\mu = [(V^2 - m_K^2 - m_\mu^2)^2/4m_K^2 - m_\mu^2]^{1/2}.$$

The 490 events in our experimental sample were divided into 18 bins as shown in Table III. Weights were calculated for each of 20 000 Monte Carlo events using the expression for ρ and different values of the parameters $\xi(0)$ and λ_+. In each case the sum of the weights was normalized to 490, and their distribution throughout the 18 bins was compared with the distribution of experimental events by calculating χ^2. The numbers in parentheses in Table III represent the sums of weights using the values of $\xi(0)$ and λ_+ which gave the lowest χ^2. These values are $\xi(0) = -0.8$, $\lambda_+ = 0.025$. The χ^2 is 19.4 for 15 degrees of freedom. The corresponding value of λ_0 as calculated from Eq. (1.5) is -0.04. The contours on the $\xi(0)$-λ_+ plane, corresponding to 1, 2, and 3 standard deviations from this minimum are shown in Fig. 4(a). Figure 4(b) shows the same contours on the λ_0-λ_+ plane.

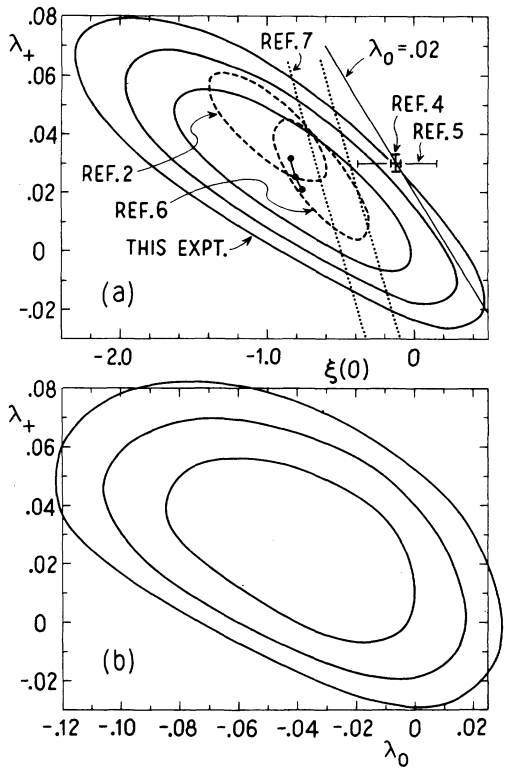

FIG. 4. The solid lines give the result of this experiment (a) in terms of λ_+, $\xi(0)$, and (b) in terms of λ_+, λ_0. The three contours represent 1σ, 2σ, and 3σ. Also shown in (a) (broken lines) are the results of other experiments: the compilations of Chounet and Gaillard (Ref. 2), Ankenbrandt *et al.* (Ref. 6), Sandweiss *et al.* (Ref. 7), Donaldson *et al.* (Ref. 4), and Chiang *et al.* (Ref. 5). The effect on the result of misestimating the stray γ impurity is indicated by the solid circles (see text).

In Figs. 5(a) and 5(b) we show the distribution of events as a function of V and $\cos\beta$, respectively. The histograms represent the experimental data. The solid circles represent the Monte Carlo data using the values of $\xi(0)$ and λ_+ corresponding to our lowest χ^2.

We have investigated the effect of misestimating the proportions of impurities in our sample. Our values of $\xi(0)$ and λ_+ are very insensitive to the

TABLE III. Division of the 490 events into 18 bins. The numbers in parentheses represent the sums of weights using $\xi(0) = -0.8$, $\lambda_+ = 0.025$.

V (GeV) \ $\cos\beta$	−1.0–0	0–0.25	0.25–0.5	0.5–0.75	0.75–1.0
0.175–0.225	17(21.58)	17(22.85)		18(20.23)	
0.250–0.275	30(40.45)	23(17.70)	18(21.39)	19(24.64)	20(22.40)
0.275–0.300	58(50.70)	20(21.93)	30(25.54)	35(32.80)	32(30.56)
0.300–0.325	50(43.67)	24(18.54)	16(23.35)	35(26.59)	28(25.08)

fraction of $K_{\pi 2}$ decays in flight. This is because these contribute no events in the region $\cos\beta \sim -1$. Hence the slope of the $\cos\beta$ distribution is not affected much by reasonably small quantities of this impurity. It is the slope of the $\cos\beta$ distribution which is most sensitive to the values of $\xi(0)$ and λ_+. On the other hand, $K_{\mu 3}$ decays with one stray γ ray do contribute quite strongly to the region $\cos\beta \sim -1$. We therefore determined how our best values for $\xi(0)$ and λ_+ changed as our estimate of this impurity changed. The results are indicated in Fig. 4 by the three solid circles, the central one corresponding to our best estimate of the stray γ impurity (2.6%), the upper circle to a 1% impurity, and the lower one to a 3.7% impurity. The method of obtaining these bounds is explained in Sec. II E.

III. REMARKS ON THE RESULT

Our result is in good agreement with a previous experiment performed by Haidt *et al.*[11] using the same technique. Their result is the major part of a compilation by Chounet, Gaillard, and Gaillard[2] which is shown in Fig. 3(a). Also shown is a result obtained by Ankenbrandt *et al.*[6] from an analysis of K^+ decays at rest using spark chambers. All three of these results are in very good agreement with one another and indicate a value of $\lambda_+ \approx 0.03 \pm 0.01$ and a value of $\xi(0) \approx -0.8 \pm 0.25$. These values are consistent with the result of a recent experiment by Sandweiss *et al.*[7] in which the polarization of the muons from $K^0_{\mu 3}$ decays was analyzed. They found $\xi(0) = -0.385 \pm 0.105 - 6\lambda_+$.

However, all of these results are in disagreement with the most appealing theoretical model, which predicts a value $\lambda_0 \sim 0.02$. This is demonstrated in Fig. 3(a), where we show the locus corresponding to $\lambda_0 = 0.02$. Furthermore, a recent experiment by Donaldson *et al.*[4] in which 1.6×10^6 $K^0_{\mu 3}$ decays were analyzed found a value of λ_0 in precise agreement with this prediction. The disagreement between this experiment and the others mentioned above is quite stark. Even our own result, which, statistically, is the weakest of the group, is a full 3.2 standard deviations out of agreement with the result of Donaldson *et al.*

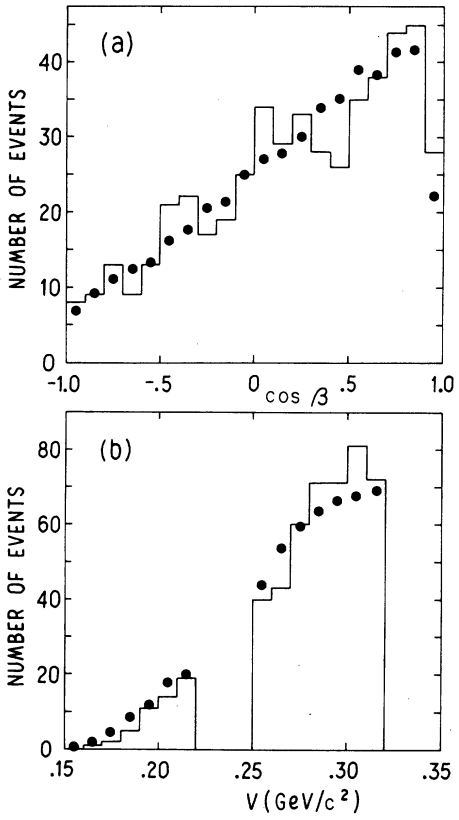

FIG. 5. Histograms of the quantities $\cos\beta$ and V. β is the angle between the pion and muon in the rest frame of the π-ν system. V is the invariant mass of the π-ν system, in GeV/c^2. The solid circles are the predictions of the Monte Carlo program for our most likely values of $\xi(0)$ and λ_+.

ACKNOWLEDGMENTS

We would like to thank the staff of the Argonne National Laboratory for the operation of the ZGS and the other facilities of the laboratory, especially V. Sevcik for the operation of the bubble chamber. We also wish to thank Professor J. Chapman of the University of Michigan for his invaluable help in setting up the on-line measuring system, and Dr. C. T. Murphy, now with NAL, for his equally important work on the geometry program SHAPE.

†Work supported in part by the U. S. Atomic Energy Commission.

[1] J. D. Jackson, in *Elementary Particle Physics and Field Theory, Brandeis Summer Institute, 1962 Lectures in Theoretical Physics*, edited by K. W. Ford (Benjamin, New York, 1963), Vol. 1, p. 263.

[2] L. M. Chounet, J. M. Gaillard, and M. K. Gaillard, Phys. Rep. 4C, 199 (1972).

[3] C. Callan and S. B. Treiman, Phys. Rev. Lett. 16, 153 (1966); M. Suzuki, *ibid.* 16, 212 (1966); V. S. Mathur, S. Okubo, and L. K. Pandit, *ibid.* 16, 371 (1966).

[4] G. Donaldson, D. Fryberger, D. Hitlin, J. Liu, B. Meyer, R. Piccioni, A. Rotherberg, D. Uggla, S. Wojcicki, and D. Dorfan, Phys. Rev. Lett. 31, 337 (1973).

[5] I.-H. Chiang, J. L. Rosen, S. Shapiro, R. Handler,

S. Olsen, and L. Pondrum, Phys. Rev. D 6, 1254 (1972).
[6]C. Ankenbrandt, R. Larsen, L. Leipuner, L. Smith, F. Shively, R. Stefanski, R. Adair, H. Kasha, S. Merlan, R. Turner, and P. Wanderer, Phys. Rev. Lett. 28, 1472 (1972).
[7]J. Sandweiss, J. Sunderland, W. Turner, W. Willis, and L. Keller, Phys. Rev. Lett. 30, 1002 (1973).
[8]B. P. Roe, D. Sinclair, and J. C. VanderVelde, in *Proceedings of the Twelfth International Conference on High Energy Physics, Dubna, 1964,* edited by Ya. A. Smorodinskii *et al.* (Atomizdat, Moscow, 1966), Vol. 2, p. 478.
[9]Particle Data Group, Rev. Mod. Phys. 45, S1 (1973).
[10]S. L. Maratek and S. P. Rosen, Phys. Lett. 29B, 497 (1969).
[11]D. Haidt *et al.* (X2 Collaboration), Phys. Rev. Lett. 29B, 691 (1969).

PHYSICAL REVIEW D VOLUME 9, NUMBER 5 1 MARCH 1974

Further measurements of forward-charged-pion electroproduction at large k^2 *

C. J. Bebek, C. N. Brown, M. Herzlinger, S. Holmes, C. A. Lichtenstein, F. M. Pipkin, and L. K. Sisterson
Cyclotron Laboratory, Harvard University, Cambridge, Massachusetts 02138

D. Andrews,† K. Berkelman, D. G. Cassel, and D. L. Hartill
Laboratory of Nuclear Studies, Cornell University, Ithaca, New York 14850

(Received 23 October 1973)

Measurements of the electroproduction reaction $e^- + p \to e^- + \pi^+ + n$ carried out at the Wilson Synchrotron Laboratory are reported. For fixed virtual photon-hadron center-of-mass energy, $W = 2.67$ GeV, data are presented with the mass of the virtual photon, $-k^2$, centered at 0.6, 1.2, and 2.0 GeV^2. At the central $-k^2 = 1.2$ (GeV)^2 point, results are also given for $W = 2.15$ GeV. For the $W = 2.67$, $-k^2 = 1.2$ GeV^2 setting, an angular scan is presented and the longitudinal transverse-interference term is extracted. The data are compared with an electric Born-model calculation of Berends which has as its only free parameter the pion electromagnetic form factor. The theory is used to extract new results for the pion form factor up to $-k^2 = 2.0$ GeV^2.

I. INTRODUCTION

In recent years the pion electroproduction reaction

$$e^- + p \to e^- + \pi^+ + n \tag{1}$$

has been studied intensively.[1-4] This reaction has generated interest for two closely related reasons. First, it has been observed that for small momentum transfer, the electric Born model gives a more than adequate description of reaction (1) and of the equivalent photoproduction reaction[5]

$$\gamma + p \to \pi^+ + n. \tag{2}$$

Second, if as suggested by the success of the electric Born model the dominant contribution is due to one-pion exchange, reaction (1) gives a direct measure of the pion electromagnetic form factor in the spacelike region.[6]

In this paper we present new measurements of pion electroproduction at higher values of $-k^2$ (the square of the mass of the virtual photon) and of W (the total center-of-mass energy of the virtual photon-proton system). Measurements were also made at the same k^2 and different W so as to study the dependence on the minimum momentum transfer. The measurements are compared with the predictions of the electric Born model and found to be in good agreement for small momentum transfer. The data at zero degrees are used to determine the pion form factor for $-k^2$ up to 2 GeV^2.

These measurements represent a continuation of similar measurements at lower energies by some members of the group. Hence, we will rely on the previous report (Ref. 2) to supply the background for the kinematics, phenomenology, and theoretical ideas needed in applying the electric Born model to our results.

II. EXPERIMENT

This experiment was performed at the Wilson Electron Synchrotron. Figure 1 gives a schematic view of the apparatus. A beam of 9.6-GeV electrons was incident on a 12.7-cm-long liquid hydrogen target. An inelastically scattered electron was detected in the Cornell 10-GeV spectrometer. A